

**APPLICATION OF THE METHOD OF FUNDAMENTAL SOLUTIONS AND
THE RADIAL BASIS FUNCTIONS FOR LAMINAR FLOW AND HEAT TRANSFER
IN INTERNALLY CORRUGATED TUBES**

Kołodziej J.A.* and Grabski J.K.

*Author for correspondence

Institute of Applied Mechanics
Department of Mechanical Engineering and Management,
Poznan University of Technology,
ul. Jana Pawła II 24, 60-965 Poznań,
Poland,
E-mail: jan.kolodziej@put.poznan.pl

ABSTRACT

Heat transfer characteristics for a laminar fully developed flow in an internally corrugated circular tube with axially uniform heat flux with peripherally uniform temperature are obtained using the method of fundamental solution and the radial basis functions. The internal shape of the tube is modelled by cosine function. The nonlinear governing equation of temperature field problem was converted into the hierarchy of non-homogenous problems using the Picard iteration method. The non-homogenous part of the equation was interpolated using the radial basis functions. On each iteration step the solution of the governing equation consists of general solution as linear combination of fundamental solutions and particular solution. Boundary conditions were satisfied using the boundary collocation method. The results of the numerical experiments, that are velocity profiles, temperature field, friction factor, Nusselt number, errors of method were presented.

INTRODUCTION

Heat transfer at fully developed steady laminar flow in circular pipes belongs to the classical problems in heat transfer analysis {[1], chapter 8}. Usually the authors consider heat transfer at constant surface heat flux or constant surface temperature. In literature one can find considerations related to heat transfer at fully developed steady laminar flow in non-circular conduits. In paper [2] square conduct was considered by means of point matching method. Flow and heat transfer characteristics in corrugated ducts confined by sinusoidal and arc curves were considered in paper [3] using finite difference technique. The numerical results for triangular, sine, rhombic and trapezoidal ducts are given in paper [4], where author use least-squares matching techniques. In paper [5] analytical-numerical method based on Gram-Schmidt orthonormalization

was used and as an example ducts of circular segment cross section were considered. The effects of duct shape on the heat transfer at fully developed laminar flow were considered in paper [6].

One of non-circular conduits important from practical standpoint of heat transfer is an internal finned tubes. The flow and heat transfer characteristics investigations have been carried out for several finned geometries under various physical and operating conditions. In this paper review other papers and our analysis are limited only to laminar and fully developed flow.

In papers [8] and [10] only fully developed laminar flow was considered in finned tubes. In paper [8] authors using finite element method consider tubes with short triangularly shaped fins. Whereas in paper [10] flow region was divided in two sub-regions in which governing equation and some boundary conditions are fulfilled exactly and only matching velocity and its normal derivatives between sub-regions are fulfilled approximately.

The theoretical analysis of laminar flow and heat transfer in internally finned tubes was considered in papers [7], [9], [11-29]. Moreover, in paper [28] authors present the experimental verification of theoretical analysis. The shapes of the cross sections of the tube considered in these papers are given in Figure 1. To the best of our knowledge as of yet the internally corrugated tubes, presented in Figure 2, haven't been considered in the literature. Fully developed laminar flow and heat transfer in such tubes is the subject of this paper.

In the aforementioned papers for the numerical analysis of laminar flow and heat transfer in internally finned tubes traditional mesh method namely: finite element method ([9], [15], [16], [17], [18], [25], [26], [27], [29]), finite difference method ([11], [12], [13], [18], [28]), finite volume method ([14], [20], [21], [23], [24]) were used. In the last decades the

meshless methods became more and more popular because they do not need a mesh. One of such meshless methods is the method of fundamental solutions (MFS). The advantage of this method is its very easy implementation. The MFS was first proposed by the Georgian researchers Kupradze and Aleksidze [30-31]. Its numerical implementation was carried out by Mathon and Johnston [32]. The mathematical analysis (convergence and stability) of this method was considered in [34-38]. The comprehensive reviews of the MFS for various applications can be found in [39-42].

The purpose of the present paper is application of the MFS for laminar flow and heat transfer in the internally corrugated tubes.

NOMENCLATURE

a	[m]	amplitude of the corrugations
A	[-]	dimensionless amplitude of the corrugations
f	[-]	friction factor
M	[-]	number of interpolation points
n_r	[-]	number of corrugations
N_{ct}	[-]	number of collocation points for the heat flow problem
N_{cv}	[-]	number of collocation points for the fluid flow problem
N_{stf}	[-]	number of source points for the heat flow problem on the pseudo-boundary for region of the fluid Ω_1
N_{stw}	[-]	number of source points for the heat flow problem on the pseudo-boundary for region of the wall Ω_2
N_{sv}	[-]	number of source points for the fluid flow problem
Nu	[-]	Nusselt number
p	[Pa]	Pressure
P	[-]	dimensionless wetted perimeter
r	[m]	cylindrical coordinate
R	[-]	dimensionless cylindrical coordinate
r_c	[m]	average inner radius of the tube
R_c	[-]	dimensionless average inner radius of the tube
r_i	[m]	inner radius of the tube
R_i	[-]	dimensionless inner radius of the tube
r_o	[m]	outer radius of the tube
R_o	[-]	dimensionless outer radius of the tube
Re	[-]	Reynolds number
Stf	[-]	dimensionless distance between pseudo-boundary and boundary of region Ω_1 (fluid) for the heat flow problem
Stw	[-]	dimensionless distance between pseudo-boundary and boundary of region Ω_2 (wall) for the heat flow problem
Sv	[-]	dimensionless distance between pseudo-boundary and boundary for the fluid flow problem
w	[m]	axial velocity
W	[-]	dimensionless axial velocity
X	[-]	dimensionless Cartesian coordinate
Y	[-]	dimensionless Cartesian coordinate
z	[m]	cylindrical coordinate
Special characters		
γ	[-]	angle of the repeated element of the tube
θ	[-]	angle in cylindrical coordinate system
θ_f	[-]	dimensionless temperature of the fluid
θ_w	[-]	dimensionless temperature of the wall
μ	[Pa·s]	dynamic viscosity
φ		form of radial basis function
Φ	[-]	additional function
ψ		particular solution for radial basis function for Laplace operator
Ω_1		region of the fluid
Ω_2		region of the wall
Subscripts		
av		Average
f		Fluid
g		general solution
p		particular solution
w		wall
Superscripts		
(i)		iteration step

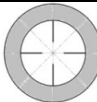
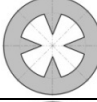
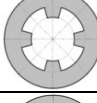
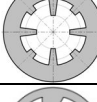
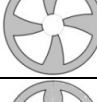
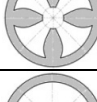
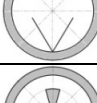
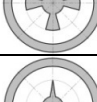


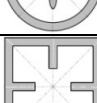
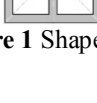
Shape of cross-section	Papers
	[7], [12], [14], [21], [22]
	[8], [9], [22], [23]
	[10], [11], [13], [19]
	[20]
	[16]
	[15], [17], [18]
	[22]
	[25]
	[27]
	[29]
	[26]
	[24]

Figure 1 Shapes of cross section of the tube considered in the previous papers

STATEMENT OF THE PROBLEM

The present paper provides solution of the momentum and energy equation for steady, incompressible laminar flow in internally corrugated tube. A typical cross section of the corrugated tube is depicted in Figure 2.

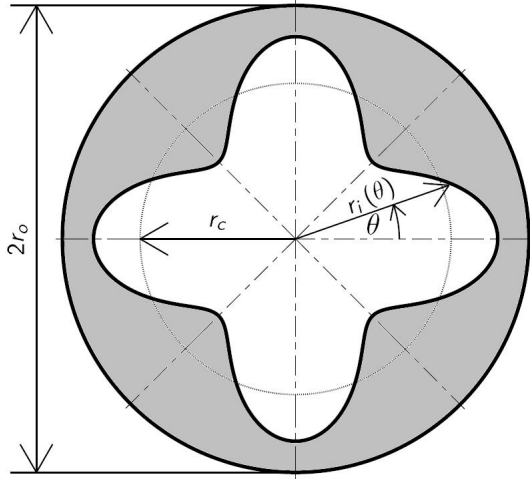


Figure 2 Typical cross-section of the corrugated tube (for number of corrugations $n_f = 4$)

Shape of the wall of the tube is described by two radiuses: constant outer radius r_o and inner radius r_i which is given by the following formula:

$$r_i(\theta) = r_c + a \cdot \cos\left(\frac{\pi\theta}{\gamma}\right) \quad (1)$$

where r_c is the „average“ inner radius of the tube, a is the amplitude of corrugations, γ is the angle of the repeated element of the tube, which can be given by:

$$\gamma = \frac{\pi}{n_f} \quad (2)$$

where n_f is the number of corrugations.

Moreover the outer radius of the tube r_o should fulfil the following condition:

$$r_o > r_c + a \quad (3)$$

Introducing the dimensionless quantities:

$$R_o = \frac{r_o}{r_c}, \quad R_i = \frac{r_i}{r_c}, \quad R_c = \frac{r_c}{r_c} = 1, \quad A = \frac{a}{r_c} \quad (4)$$

equation (1) becomes

$$R_i(\theta) = 1 + A \cdot \cos\left(\frac{\pi\theta}{\gamma}\right) \quad (5)$$

These dimensionless radiuses are shown in Figure 3 where the repeated element of the tube is presented. Region of the fluid is signed as Ω_1 whereas region of the wall is signed as Ω_2 .

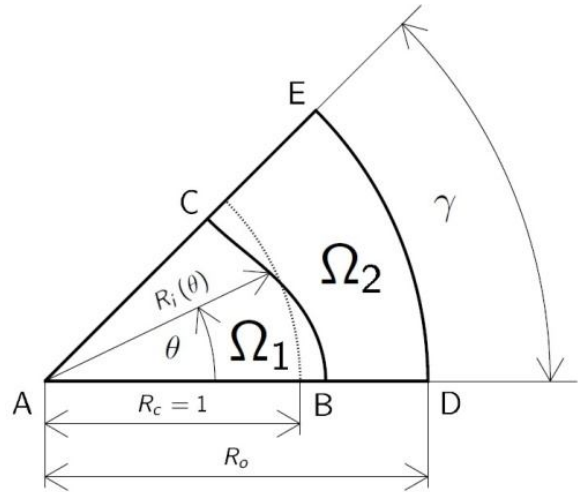


Figure 3 The repeated element of the tube with dimensionless radiuses

Governing momentum equation

Steady fully developed laminar flow of incompressible Newtonian fluid in the tube with constant cross section is governed by equation in the form (in cylindrical coordinates r, θ, z):

$$\frac{\partial^2 w(r, \theta)}{\partial r^2} + \frac{1}{r} \frac{\partial w(r, \theta)}{\partial r} + \frac{1}{r^2} \frac{\partial^2 w(r, \theta)}{\partial \theta^2} = \frac{1}{\mu} \frac{dp}{dz} \quad (6)$$

where $w(r, \theta)$ is the axial velocity, μ is the dynamic viscosity, dp/dz is the constant pressure gradient in z -direction.

Let's introduce the following dimensionless variables:

$$R = \frac{r}{r_c}, \quad W(R, \theta) = \frac{w(r, \theta)}{\frac{r_c^2}{\mu} \frac{dp}{dz}} \quad (7)$$

Now, the governing equation (6) takes the following form:

$$\frac{\partial^2 W(R, \theta)}{\partial R^2} + \frac{1}{R} \frac{\partial W(R, \theta)}{\partial R} + \frac{1}{R^2} \frac{\partial^2 W(R, \theta)}{\partial \theta^2} = -1 \quad (8)$$

Introducing additional function:

$$\Phi(R, \theta) = W(R, \theta) + \frac{1}{4}(R^2 - 1) \quad (9)$$

equation (8) takes the following form (Laplace equation):

$$\frac{\partial^2 \Phi(R, \theta)}{\partial R^2} + \frac{1}{R} \frac{\partial \Phi(R, \theta)}{\partial R} + \frac{1}{R^2} \frac{\partial^2 \Phi(R, \theta)}{\partial \theta^2} = 0 \quad (10)$$

For determination of fluid velocity in region Ω_1 , governed by equation (8) the following boundary conditions should be used (resulting from symmetry of the problem and non-slip on solid boundary):

$$\frac{\partial W(R, \theta)}{\partial \theta} = 0 \quad \text{on boundary } AB \text{ and } CA \quad (11)$$

$$W(R, \theta) = 0 \quad \text{on boundary } BC \quad (12)$$

For equation (10) these boundary conditions take the forms:

$$\frac{\partial \Phi(R, \theta)}{\partial \theta} = 0 \text{ on boundary } AB \text{ and } CA \quad (13)$$

$$\Phi(R, \theta) = \frac{1}{4}(R^2 - 1) \text{ on boundary } BC \quad (14)$$

Dimensionless average fluid velocity W_{av} is defined by:

$$W_{av} = \frac{\int_{\Omega_1} W d\Omega_1}{\int_{\Omega_1} d\Omega_1} \quad (15)$$

Product of friction factor f and Reynolds number Re can be expressed as:

$$f Re = \frac{8\gamma^2(1 + 0.5A^2)^2}{W_{av} P^2} \quad (16)$$

where P is dimensionless wetted perimeter:

$$P = \int_0^\gamma \sqrt{\left(1 + A \cos\left(\frac{\pi\theta}{\gamma}\right)\right)^2 + \left(A \frac{\pi}{\gamma} \sin\left(\frac{\pi\theta}{\gamma}\right)\right)^2} d\theta \quad (17)$$

Governing energy equation

The analysis is based on the following assumptions:

- 1) heat flux through the outer boundary of the tube on unit length of the tube is constant;
- 2) heat transfer in axial direction can be neglected;
- 3) temperature profile in cross sections of the tube is steady (heat transfer between the wall and the fluid is fully developed).

On the base of above assumption energy equation has form:

$$\frac{\partial^2 \theta_f(R, \theta)}{\partial R^2} + \frac{1}{R} \frac{\partial \theta_f(R, \theta)}{\partial R} + \frac{1}{R^2} \frac{\partial^2 \theta_f(R, \theta)}{\partial \theta^2} = \frac{f Re}{4} \cdot W(R, \theta) \frac{\theta_f(R, \theta)}{\theta_{f av}} \quad (18)$$

where $\theta_f(R, \theta)$ is dimensionless temperature of the fluid in region Ω_1 , which is defined as:

$$\theta_f(R, \theta) = \frac{(T_f(r, \theta) - T_o) k_f}{q_{av} r_c} \quad (19)$$

where $T_f(r, \theta)$ is temperature in the point (r, θ) , T_o is temperature on the wall DE, k_f is the thermal conductivity of fluid, q_{av} is average heat flux through external surface of the tube.

Average dimensionless temperature of fluid is defined as:

$$\theta_{f av} = \frac{\int_{\Omega_1} \theta_f W d\Omega_1}{\int_{\Omega_1} W d\Omega_1} \quad (20)$$

and Nusselt number is obtained as:

$$Nu = -\frac{2}{\theta_{f av}} \quad (21)$$

The governing equation for steady heat transfer in the wall of the tube has the form:

$$\frac{\partial^2 \theta_w(R, \theta)}{\partial R^2} + \frac{1}{R} \frac{\partial \theta_w(R, \theta)}{\partial R} + \frac{1}{R^2} \frac{\partial^2 \theta_w(R, \theta)}{\partial \theta^2} = 0 \quad (22)$$

where $\theta_w(R, \theta)$ is dimensionless temperature of the wall in region Ω_2 . Definition of $\theta_w(R, \theta)$ is similar to the definition of dimensionless temperature of the fluid $\theta_f(R, \theta)$ (equation (18)) but instead of $T_f(r, \theta)$ there is wall temperature $T_w(r, \theta)$ and instead of k_f there is thermal conductivity of the wall material k_w .

For heat transfer governed by equation (17) for region Ω_1 and equation (20) for region Ω_2 the following boundary conditions are used:

$$\frac{\partial \theta_f(R, \theta)}{\partial \theta} = 0 \text{ on boundary } AB \text{ and } CA \quad (23)$$

$$\left. \begin{aligned} \theta_f(R, \theta) &= \theta_w(R, \theta) \\ \frac{\partial \theta_f(R, \theta)}{\partial n} &= K \frac{\partial \theta_w(R, \theta)}{\partial n} \end{aligned} \right\} \text{ on boundary } BC \quad (24)$$

$$\frac{\partial \theta_w(R, \theta)}{\partial \theta} = 0 \text{ on boundary } BD \text{ and } CE \quad (25)$$

$$\theta_w(R, \theta) = 0 \text{ on boundary } BC \quad (26)$$

where $K = k_w/k_f$ is dimensionless thermal conductivity of wall, n is normal direction.

These boundary conditions result from the symmetry of the problem, continuity temperature and heat flux on boundary BC and given temperature T_o on the outer wall of the tube.

Boundary value problem of flow and heat transfer in corrugated tube is formulated by coupled system of equations (10), (18), (22) with boundary conditions (13-14), (23-26). Problem is non-linear due to equation (18) in which on the right-hand side the average value of fluid temperature is unknown.

THE PROPOSED METHOD OF SOLUTION

The proposed method of solution for the fluid flow problem

Fluid flow problem is governed by non-homogeneous equation (8) transformed to Laplace equation (10) with unknown function Φ . Using the MFS the approximate solution of equation (10) takes the following form:

$$\Phi(X, Y) = \sum_{j=1}^{Nsv} c_j \ln(r_j) \quad (27)$$

where Nsv is the number of source points on pseudo-boundary, c_j ($j = 1, 2, \dots, Nsv$) are unknown coefficients, r_j is distance between the point (X, Y) and the source point (X_j, Y_j) :

$$r_j = \sqrt{(X - X_j)^2 + (Y - Y_j)^2} \quad (28)$$

The pseudo-boundary has similar shape as the boundary of the considered region and is located in distance Sv from the boundary of region Ω_1 .

The unknown coefficients c_j ($j = 1, 2, \dots, Nsv$) are calculated using the boundary collocation method at Ncv collocation points which are located on the boundary of region Ω_1 [43]. The distribution of source points and collocation points is depicted in Figure 4.

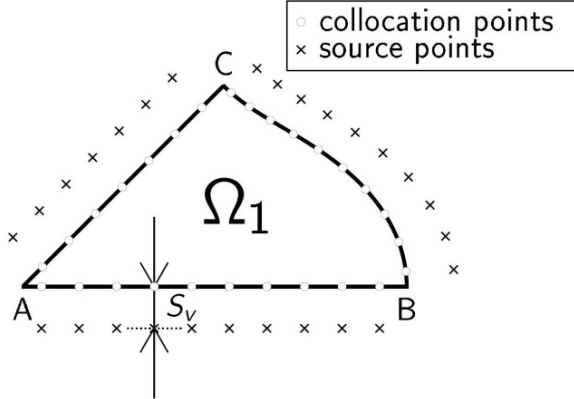


Figure 4 Distribution of source points and collocation points for the fluid flow problem

The proposed method of solution for the heat flow problem

In order to solve the problem of heat flow in the region Ω_1 described by nonlinear equation (18) the Picard iteration method is used. In the method the value of temperature from previous iteration step is used in the right-hand side of equation (18). This way the nonlinear equation (18) is transformed into the hierarchy of non-homogenous equations in the following form:

$$\frac{\partial^2 \theta_f^{(i)}(R, \theta)}{\partial R^2} + \frac{1}{R} \frac{\partial \theta_f^{(i)}(R, \theta)}{\partial R} + \frac{1}{R^2} \frac{\partial^2 \theta_f^{(i)}(R, \theta)}{\partial \theta^2} = f \operatorname{Re} \cdot W(R, \theta) \frac{\theta_f^{(i-1)}(R, \theta)}{\theta_f^{(i-1)}(R, \theta)} \quad (29)$$

where i is iteration step number. The right-hand side of the above equation in i -th iteration is signed by function $g^{(i)}$, which can be interpolated using radial basis functions (RBFs) at M interpolation points which are located inside of region Ω_1 . At any point (X, Y) in region Ω_1 function $g^{(i)}(X, Y)$ can be expressed by:

$$g^{(i)}(X, Y) = \sum_{m=1}^M \alpha_m \varphi(r_m) \quad (30)$$

where φ is assumed form of RBF, r_m ($m = 1, 2, \dots, M$) is distance between the point (X, Y) and m -th interpolation point (X_m, Y_m) :

$$r_m = \sqrt{(X - X_m)^2 + (Y - Y_m)^2} \quad (31)$$

In order to determine the unknown coefficients α_m the following system of equations should be solved:

$$g^{(i)}(X_j, Y_j) = \sum_{m=1}^M \alpha_m \varphi(r_{jm}) \quad 1 \leq j \leq M \quad (32)$$

The solution of the non-homogenous equation (29) in i -th iteration step has the form:

$$\theta_f^{(i)}(X, Y) = \theta_{fg}^{(i)}(X, Y) + \theta_{fp}^{(i)}(X, Y) \quad (33)$$

where θ_{fg} is general solution of homogenous equation, whereas θ_{fp} is particular solution of non-homogenous equation.

The particular solution has the following form:

$$\theta_{fp}^{(i)}(X, Y) = \sum_{m=1}^M \alpha_m \psi(r_m) \quad (34)$$

where ψ is the particular solution for the assumed form of the RBF for Laplace operator:

$$\nabla^2 \psi(r_m) = \varphi(r_m) \quad (35)$$

Coefficients α_m ($m = 1, 2, \dots, M$) in equation (34) are known from interpolation of the right-hand side of equation (29) by solving system of equations (32).

In the paper multiquadric function (MQ) was used as RBF. The MQ has the following form:

$$\varphi(r_m) = \sqrt{r_m^2 + c^2} \quad (36)$$

where c is the shape factor. The particular solution for MQ for Laplace operator has the following form:

$$\psi(r_m) = -\frac{1}{3} c^3 \ln \left(c \sqrt{r_m^2 + c^2} + c^2 \right) + \frac{1}{9} (r_m^2 + 4c^2) \sqrt{r_m^2 + c^2} \quad (37)$$

The general solution in i -th iteration step is the solution of the homogenous equation:

$$\nabla^2 \theta_{fg}^{(i)} = 0 \quad (38)$$

The solution of above equation using MFS can be written as a linear combination of fundamental solutions:

$$\theta_{fp}^{(i)}(X, Y) = \sum_{j=1}^{Nstf} d_j \ln(r_j) \quad (39)$$

where $Nstf$ is the number of source points. The source points are located on the pseudo-boundary which is in distance Stf from the boundary of considered region Ω_1 .

Using the MFS the approximate solution of equation (22) has a similar form:

$$\theta_w(X, Y) = \sum_{n=1}^{Nstw} h_n \ln(r_n) \quad (40)$$

where $Nstw$ denotes number of source points. The pseudo-boundary is located in distance Stw from the boundary of the considered region Ω_2 .

Coefficients d_j ($j = 1, 2, \dots, Nstf$) and h_n ($n = 1, 2, \dots, Nstw$) can be calculated using the boundary collocation method in Nct collocation points. The distribution of the interpolation points inside the region Ω_1 , collocation points on the boundaries of the considered regions Ω_1 and Ω_2 and source points on pseudo-boundaries for the heat flow problem is illustrated in Figure 5.

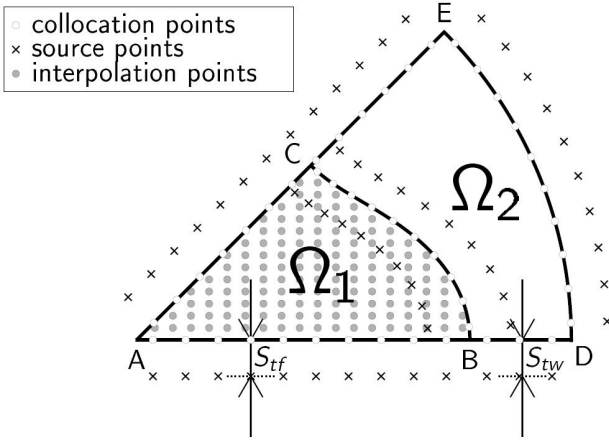


Figure 5 Distribution of source points, collocation points and interpolation points for the heat flow problem

NUMERICAL ALGORITHM OF THE PROPOSED METHOD

In Table 1 subsequent steps of the proposed method are presented.

Table 1 Numerical algorithm of the proposed method

STEP 1	Input dimensionless parameters describing the considered region: γ , A , R_o and dimensionless thermal conductivity of wall K .
STEP 2	Input parameters of the proposed method: for the fluid flow problem (Nsv , Sv) and for the heat flow problem ($Nstf$, $Nstw$, M , Stf , Stw , c).
STEP 3	Solve the problem described by equation (10) and boundary conditions (13-14).
STEP 4	Calculate dimensionless average fluid velocity W_{av} and product of fRe .
STEP 5	Take $\theta_f^{(0)}/\theta_{f_{sr}}^{(0)} = 1$ in the whole region Ω_1 and $i = 1$.
STEP 6	Interpolate the right-hand side of equation (29) using RBFs.
STEP 7	Fulfill the boundary conditions (23-26) for the region Ω_1 and Ω_2 .
STEP 8	Calculate average fluid temperature $\theta_{f_{av}}$.
STEP 9	Check end condition for iteration process: If $\delta < tol$ STOP If $\delta \geq tol$ take $i = i + 1$ and go to STEP 6 (δ – error of iteration process convergence, tol – assumed tolerance of δ)

Dimensionless average fluid velocity W_{av} and dimensionless average fluid temperature θ_{av} are calculated numerically.

In order to fulfil boundary conditions (in STEP 3 and STEP 7) two methods can be applied. If number of source points equals number of collocation points than the system of equations is solved using Gaussian elimination. If number of collocation points is greater than number of source points the system of equations is solved by means of singular value decomposition (SVD) method.

RESULTS

Numerical experiments were conducted for some selected parameters of considered region ($n_f = \{3; 4; 5; 6\}$; $A = \{0,1; 0,2; 0,3; 0,4\}$). In each of all analyzed problems dimensionless thermal conductivity K was equaled 50 and dimensionless outer radius of the tube R_o was equaled 1,5.

In Figure 6-9 equivelocity lines are presented for the same number of corrugation ($n_f = 3$) and different dimensionless amplitudes of corrugation ($A = \{0,1; 0,2; 0,3; 0,4\}$). The corresponding values of dimensionless average fluid velocity W_{av} and product of friction factor and Reynolds number fRe are presented in Table 2. The greater the amplitude of corrugation the smaller fluid velocity (and dimensionless average velocity) and the greater product of friction factor and Reynolds number fRe .

Equivelocity lines for the same dimensionless amplitude of corrugation ($A = 0,2$) and different number of corrugations ($n_f = \{3; 4; 5; 6\}$) are presented in Figure 10-13. In Table 3 dimensionless average fluid velocity W_{av} and product of friction factor and Reynolds number fRe are summarised. The average fluid velocity W_{av} and product fRe decreases with increasing number of corrugation n_f .

In Figure 14-17 isotherms are presented for different dimensionless amplitudes of corrugation ($A = \{0,1; 0,2; 0,3; 0,4\}$) and the same number of corrugations ($n_f = 3$). The corresponding values of dimensionless average fluid temperature $\theta_{f_{av}}$ and Nusselt number Nu are summarised in Table 4. On the base of these results the following relation can be observed – the greater amplitude of the corrugation A the greater average fluid temperature and the greater Nusselt number Nu .

Isotherms for different number of corrugations ($n_f = \{3; 4; 5; 6\}$) and the same dimensionless amplitude of corrugation ($A = 0,2$) are illustrated in Figure 18-21. In Table 5 the corresponding values of dimensionless average fluid temperature $\theta_{f_{av}}$ and Nusselt number Nu are presented. One can be observed – the greater number of corrugations the greater dimensionless average fluid temperature $\theta_{f_{av}}$ and the greater Nusselt number Nu .

In Table 6 root mean square (RMS) errors of fulfilment boundary conditions for the fluid flow problem are summarised. The errors were obtained for $n_f = 3$; $A = 0,3$; $Ncv = 80$; $Nsv = 45$ and $Sv = 0,4$.

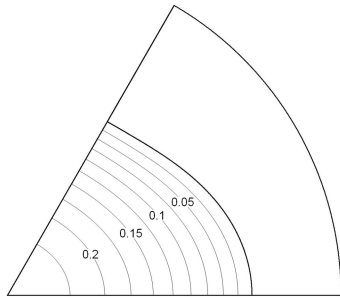


Figure 6 Equivelocity lines for $n_f=3$; $A=0,1$

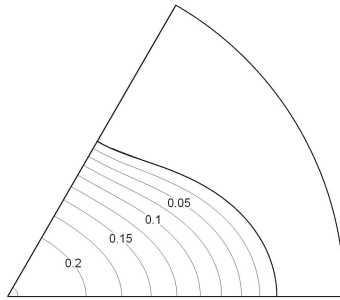


Figure 7 Equivelocity lines for $n_f=3$; $A=0,2$

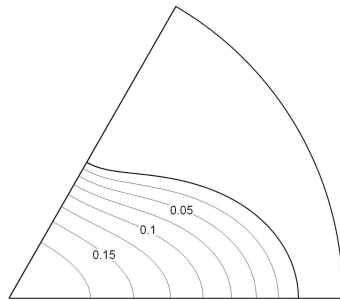


Figure 8 Equivelocity lines for $n_f=3$; $A=0,3$

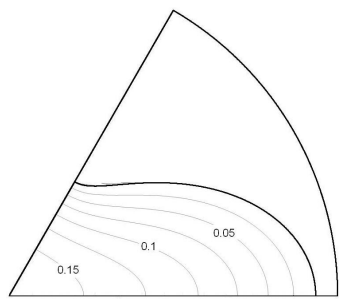


Figure 9 Equivelocity lines for $n_f=3$; $A=0,4$

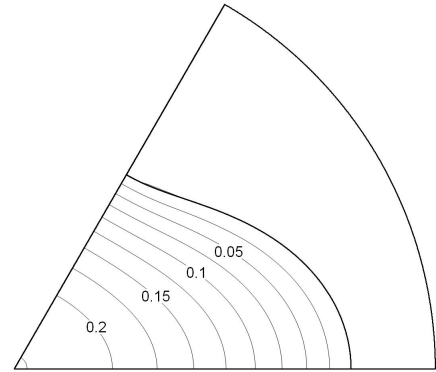


Figure 10 Equivelocity lines for $n_f=3$; $A=0,2$

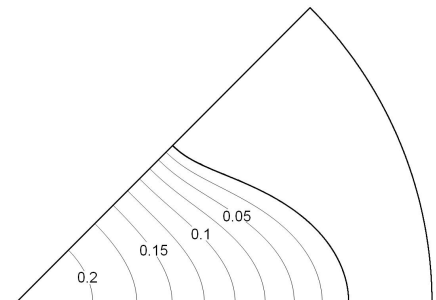


Figure 11 Equivelocity lines for $n_f=4$; $A=0,2$

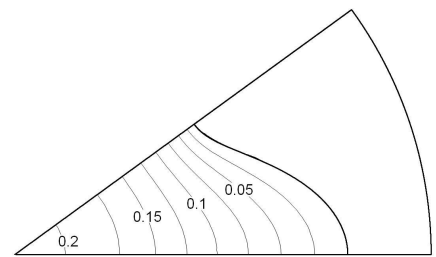


Figure 12 Equivelocity lines for $n_f=5$; $A=0,2$

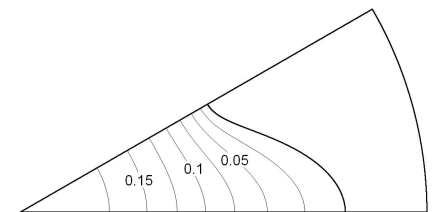


Figure 13 Equivelocity lines for $n_f=6$; $A=0,2$

Table 2 Average fluid velocity W_{av} and product $f \cdot Re$ for different values of corrugation amplitude

n_f	A	W_{av}	$f \cdot Re$
3	0,1	0,1207	64,04
	0,2	0,1092	64,66
	0,3	0,0940	66,44
	0,4	0,0785	69,83

Table 3 Average fluid velocity W_{av} and product $f \cdot Re$ for different values of corrugation amplitude

A	n_f	W_{av}	$f \cdot Re$
0,2	3	0,1092	64,66
	4	0,1017	62,26
	5	0,0946	59,41
	6	0,0845	55,83

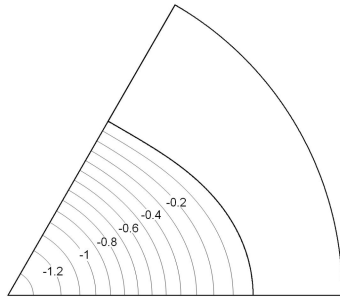


Figure 14 Isotherms for $n_f = 3$; $A = 0,1$

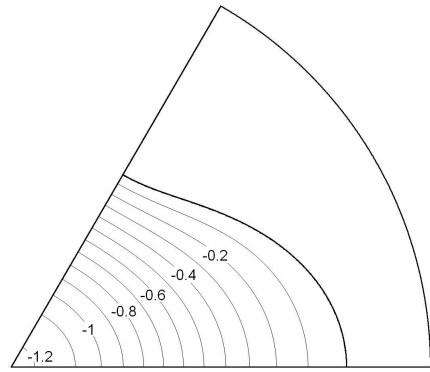


Figure 18 Isotherms for $n_f = 3$; $A = 0,2$

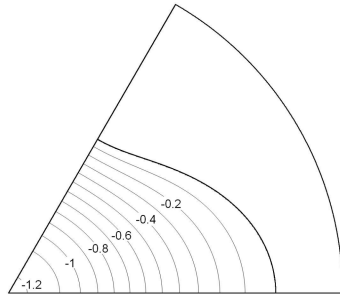


Figure 15 Isotherms for $n_f = 3$; $A = 0,2$

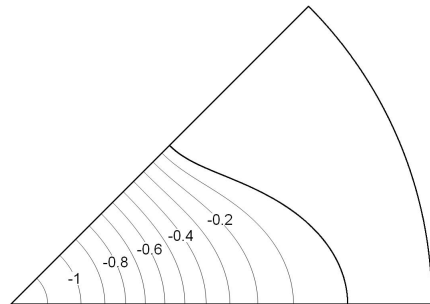


Figure 19 Isotherms for $n_f = 4$; $A = 0,2$

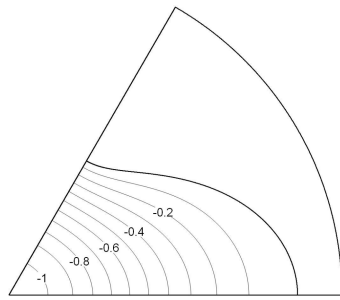


Figure 16 Isotherms for $n_f = 3$; $A = 0,3$

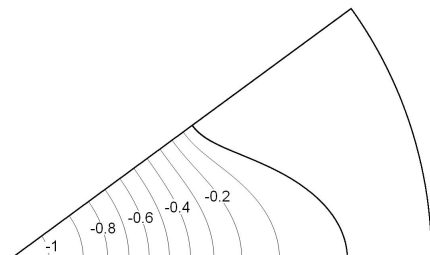


Figure 20 Isotherms for $n_f = 5$; $A = 0,2$

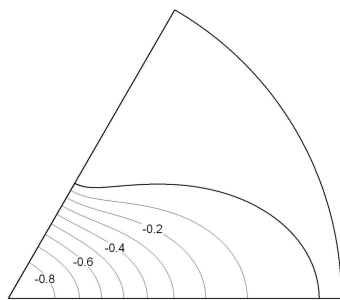


Figure 17 Isotherms for $n_f = 3$; $A = 0,4$

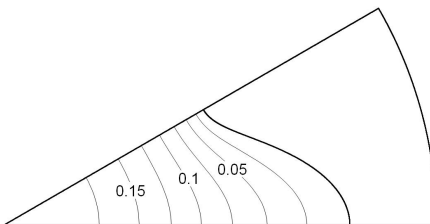


Figure 21 Isotherms for $n_f = 6$; $A = 0,2$

Table 4 Average fluid temperature $\theta_{f,av}$ and Nusselt number Nu for different values of corrugation amplitude

n_f	A	$\theta_{f,av}$	Nu
3	0,1	-0,5153	3,88
	0,2	-0,4596	4,35
	0,3	-0,3604	5,55
	0,4	-0,2581	7,75

Table 5 Average fluid temperature $\theta_{f,av}$ and Nusselt number Nu for different values of corrugation amplitude

A	n_f	$\theta_{f,av}$	Nu
0,2	3	-0,4596	4,35
	4	-0,3989	5,01
	5	-0,3526	5,67
	6	-0,3213	6,22

Table 6 RMS errors of fulfilment boundary conditions for the fluid flow problem

boundary	condition	RMS error
AB	$\frac{\partial \Phi(R, \theta)}{\partial \theta} = 0$	$8,2425 \cdot 10^{-7}$
BC	$\Phi(R, \theta) = 0$	$2,2363 \cdot 10^{-6}$
CA	$\frac{\partial \Phi(R, \theta)}{\partial \theta} = 0$	$1,2000 \cdot 10^{-5}$

The convergence of iteration process was obtained for all analysed cases. RMS errors of iteration process convergence is presented in Table 7 (example for $n_f = 3$; $A = 0,3$). The errors were obtained for $Nstf = 80$; $Nstw = 20$; $Nct = 310$; $Stf = 0,25$; $Stw = 0,4$; $M = 518$; $c = 0,1$. The RMS error of interpolation was equal $3,2118 \cdot 10^{-2}$.

Table 7 RMS errors of iteration process convergence

iteration step i	RMS error
1	$1,4257 \cdot 10^{-2}$
2	$3,3325 \cdot 10^{-3}$
3	$4,5883 \cdot 10^{-4}$
4	$1,1289 \cdot 10^{-4}$
5	$2,5741 \cdot 10^{-5}$
6	$5,9877 \cdot 10^{-6}$
7	$1,3969 \cdot 10^{-6}$
8	$3,2634 \cdot 10^{-7}$
9	$7,6278 \cdot 10^{-8}$
10	$1,7831 \cdot 10^{-8}$

The Table 8 presents RMS errors of fulfilment boundary conditions for the heat flow problem for $n_f = 3$; $A = 0,3$. The presented results were obtained for $Nstf = 80$; $Nstw = 20$; $Nct = 310$; $Stf = 0,25$; $Stw = 0,4$; $M = 518$; $c = 0,1$.

Table 8 RMS errors of fulfilment boundary conditions for the heat flow problem

boundary	condition	RMS error
AB	$\frac{\partial \theta_f(R, \theta)}{\partial \theta} = 0$	$3,7385 \cdot 10^{-6}$
CA	$\frac{\partial \theta_f(R, \theta)}{\partial \theta} = 0$	$4,2363 \cdot 10^{-6}$
BD	$\frac{\partial \theta_w(R, \theta)}{\partial \theta} = 0$	$8,9495 \cdot 10^{-7}$
DE	$\theta_w(R, \theta) = 0$	$1,0273 \cdot 10^{-6}$
CE	$\frac{\partial \theta_w(R, \theta)}{\partial \theta} = 0$	$7,7662 \cdot 10^{-7}$
BC (I condition)	$\theta_f(R, \theta) = \theta_w(R, \theta)$	$3,0033 \cdot 10^{-6}$
BC (II condition)	$\frac{\partial \theta_f(R, \theta)}{\partial n} = K \frac{\partial \theta_w(R, \theta)}{\partial n}$	$5,6437 \cdot 10^{-2}$

CONCLUSIONS

In the paper the fluid and heat flow problem was considered numerically using the MFS and RBFs. The following conclusions can be drawn from this study:

1. Product of friction factor and Reynolds number fRe increases with increasing dimensionless amplitude of corrugation A and decreases with increasing number of corrugations n_f .
2. Nusselt number Nu increases with increasing dimensionless amplitude of corrugation A and with increasing number of corrugations n_f .
3. Application of the MFS and the RBFs give satisfying results. The worse fulfilled boundary condition was the second condition on BC boundary for the heat flow problem (condition for continuity heat flux in normal direction n).

ACKNOWLEDGEMENTS

First author gratefully acknowledges the support provided this research by grant Polish NCN no. 2012/07/B/ST8/03449.

REFERENCES

- [1] Çengel, Y.A., *Heat Transfer. A Practical Approach*, McGraw-Hill, New York 2003.
- [2] Cheng, K.C., Analog solution of laminar heat transfer in noncircular ducts by Moiré method and point-matching, *Journal of Heat Transfer*, Vol. 11, 1966, pp. 172-182.
- [3] Niu, J.L., and Zhang, L.Z., Heat transfer and friction coefficients in corrugated ducts confined by sinusoidal and arc curves, *International Journal of Heat and Mass Transfer*, Vol. 45, 2002, pp. 571-578.
- [4] Shah, R.K., Laminar flow friction and forced convection heat transfer in ducts of arbitrary geometry, *International Journal of Heat and Mass Transfer*, Vol. 18, 1975, pp. 849-862.
- [5] Sparrow, E.M., and Haji-Sheikh, A., Flow and heat transfer in ducts of arbitrary shape with arbitrary thermal boundary conditions, *Journal of Heat Transfer*, Vol. 88, 1966, pp. 351-358.
- [6] Erdoğan, M.E., and Imrak, C.E., The effects of duct shape on the Nusselt number, *Mathematical and Computational Applications*, Vol. 10, 2005, pp. 79-88.
- [7] Hu, M.H., and Chang, Y.P., Optimization of finned tubes for heat transfer in laminar flow, *Journal of Heat Transfer*, Vol. 95, 1973, pp. 332-338.
- [8] Nandakumar, K., and Masliyah, J.H., Fully developed viscous flow in internally finned tubes, *Chemical Engineering Journal*, Vol. 10, 1975, pp. 113-120.
- [9] Masliyah, J.H., and Nandakumar, K., Heat transfer in internally finned tubes, *Journal of Heat Transfer*, Vol. 96, 1976, pp. 257-261.
- [10] Soliman, H.M., and Feingold, A., Analysis of Fully Developed Laminar Flow in Longitudinal Internally Finned Tubes, *Chemical Engineering Journal*, Vol. 14, 1977, pp. 119-128.
- [11] Soliman, H.M., Chau, T.S., and Trupp, A.C., Analysis of laminar heat transfer in internally finned tubes with uniform outside wall temperature, *Journal of Heat Transfer*, Vol. 102, 1980, pp. 598-604.
- [12] Ruston, I.M., and Soliman, H.M., Forced convection in the entrance region of tubes with longitudinal internal fins, *Journal of Heat Transfer*, Vol. 110, 1988, pp. 310-313.
- [13] Kettner, I.J., Degani, D., and Gutfinger, G., Numerical study of heat transfer in internally finned tubes, *Numerical Heat Transfer, Part A*, Vol. 20, 1991, pp. 159-180.

- [14] Lendeza, G.A., and Camp, A., Computation of the Nusselt number asymptotes for laminar convection flows in internally finned tubes, *International Communications in Heat and Mass Transfer*, Vol. 26, 1999, pp. 399-409.
- [15] Fabbri, G., Heat transfer optimization in internally finned tubes under laminar flow, *International Journal of Heat and Mass Transfer*, Vol. 41, 1998, pp. 1243-1253.
- [16] Fabbri, G., Optimum profiles for asymmetrical longitudinal fins in cylindrical ducts, *International Journal of Heat and Mass Transfer*, Vol. 42, 1999, pp. 511-523.
- [17] Fabbri, G., Optimum cross-section design of internally finned tubes cooled by a viscous fluid, *Control Engineering Practice*, Vol. 13, 2005, pp. 929-938.
- [18] Fabbri, G., Effect of viscous dissipation on the optimization of the heat transfer in internally finned tubes, *International Journal of Heat and Mass Transfer*, Vol. 47, 2004, pp. 3003-3015.
- [19] Alam, I., and Ghoshdastidar, P.S., A study of heat transfer effectiveness of circular tubes with internal longitudinal fins having tapered lateral profiles, *International Journal of Heat and Mass Transfer*, Vol. 45, 2002, pp. 1371-1376.
- [20] Zeitoun, O., and Hegazy, A.S., Heat transfer for laminar flow in internally finned pipes with different fin heights and uniform wall temperature, *Heat and Mass Transfer*, Vol. 40, 2004, pp. 253-259.
- [21] Al-Sarkhi, A., and Abu-Nada, E., Characteristics of forced convection heat transfer in vertical internally finned tube, *International Communications in Heat and Mass Transfer*, Vol. 32, 2005, pp. 557-564.
- [22] Dagtekin, I., Oztop, H.F., and Sahin, A.Z., An analysis of entropy generation through a circular duct with different shaped longitudinal fins for laminar flow, *International Journal of Heat and Mass Transfer*, Vol. 48, 2005, pp. 171-181.
- [23] Duplain, E., and Baliga, B.R., Computational optimization of the thermal performance of internally finned ducts, *International Journal of Heat and Mass Transfer*, Vol. 52, 2009, pp. 3929-3942.
- [24] Foong, A.J.L., Ramesh, N., and Chandratilleke, T.T., Laminar convective heat transfer in a microchannel with internal longitudinal fins, *International Journal of Thermal Sciences*, Vol. 48, 2009, pp. 1908-1913.
- [25] Syed, K.S., Iqbal, Z., and Ishaq, M., Optimal configuration of finned annulus in a double pipe with fully developed laminar flow, *Applied Thermal Engineering*, Vol. 31, 2011, pp. 1435-1446.
- [26] Iqbal, Z., Syed, K.S., and Ishaq, M., Optimal convective heat transfer in double pipe with parabolic fins, *International Journal of Heat and Mass Transfer*, Vol. 54, 2011, pp. 5415-5426.
- [27] Syed, K.S., Ishaq, M., and Bakhsh, M., Laminar convection in the annulus of a double-pipe with triangular fins, *Computers & Fluids*, Vol. 44, 2011, pp. 43-55.
- [28] Tien, W.-K., Yeh, R.-H., and Hsiao, J.-C., Numerical analysis of laminar flow and heat transfer in internally finned tubes, *Heat Transfer Engineering*, Vol. 33, 2012, pp. 957-971.
- [29] Ishaq, M., Syed, K.S., Iqbal, Z., Hassan, A., and Ali, A., DG-FEM based simulation of laminar convection in an annulus with triangular fins of different heights, *International Journal of Thermal Sciences*, Vol. 72, 2013, pp. 125-146.
- [30] Kupradze, V.D., and Aleksidze, M.A., Approximate method of solving certain boundary-value problems, *Soobsc. Akad. Nauk Gruzin. SSR*, Vol. 30, 1963, pp. 529-536 (in Russian).
- [31] Kupradze, V.D., and Aleksidze, M.A., The method of functional equations for an approximate solution of certain boundary value problems, *USSR. Comput. Math. Comput. Phys.*, Vol. 4, 1964, pp. 683-715.
- [32] Mathon, R., and Johnston, R.L., The approximate solution of elliptic boundary-value problems by fundamental solutions, *SIAM Journal on Numerical Analysis*, Vol. 14, 1977, pp. 638-650.
- [33] Bogomolny, A., Fundamental solution method for elliptic boundary value problems, *SIAM Journal on Numerical Analysis*, Vol. 22, 1985, pp. 644-669.
- [34] Katsurada, M., and Okamoto, H., The collocation points of the fundamental solution method for the potential problem, *Computers & Mathematics with Applications*, Vol. 31, 1996, pp. 123-137.
- [35] Kitagawa, T., On the numerical stability of the method of fundamental solutions applied to the Dirichlet problem, *Jap. J. Appl. Math.* 1988, Vol. 35, s. 507-518.
- [36] Katsurada, M., Asymptotic error analysis of the charge simulation method, *Journal of the Faculty of Science, University of Tokyo, Section 1A, Mathematics*, Vol. 37, 1990, pp. 635-657.
- [37] Kitagawa, T., Asymptotic stability of the fundamental solution method, *Journal of Computational and Applied Mathematics*, Vol. 38, 1991, pp. 263-269.
- [38] Katsurada, M., and Okamoto, H., A mathematical study of the charge simulation method, *Journal of the Faculty of Science, University of Tokyo, Section 1A, Mathematics*, Vol. 35, 1998, pp. 507-518.
- [39] Fairweather, G., and Karageorghis, A., The method of fundamental solutions for elliptic boundary value problems, *Advances in Computational Mathematics*, Vol. 9, 1998, pp. 69-95.
- [40] Golberg M.A., and Chen, C.S., The method of fundamental solutions for potential, Helmholtz and diffusion problems. In: Golberg, M.A., editor, *Boundary Integral Methods – Numerical and Mathematical Aspects*, Computational Mechanics Publications, Boston 1998, pp. 103-176.
- [41] Fairweather, G., Karageorghis, A., and Martin, P.A., The method of fundamental solutions for scattering and radiation problems, *Engineering Analysis with Boundary Elements*, Vol. 27, 2003, pp. 759-769.
- [42] Chen, C.S., Karageorghis, A., and Smyrlis, Y.S., *The Method of Fundamental Solutions – A Meshless Method*, Dynamic Publishers, Atlanta 2008.
- [43] Kołodziej, J.A., and Zieliński, A.P., *Boundary Collocation Techniques and their Application in Engineering*, WIT Press, Southampton 2009.